Journal of Great Lakes Research 40 (2014) 336–346

Contents lists available at ScienceDirect

Journal of Great Lakes Research

journal homepage: www.elsevier.com/locate/jglr

# Stable isotope mass balance of the Laurentian Great Lakes

Scott Jasechko [a,b,*], John J. Gibson [b,c], Thomas W.D. Edwards [a]

[a] Department of Earth and Environmental Sciences, University of Waterloo, Waterloo, ON N2L 3G1, Canada
[b] Alberta Innovates - Technology Futures, Vancouver Island Technology Park, 3-4476 Markham St., Victoria, BC V8Z 7X8, Canada
[c] Department of Geography, University of Victoria, Victoria, BC V8W 3P5, Canada

ARTICLE INFO

*Article history:*
Received 8 May 2013
Accepted 9 February 2014
Available online 18 April 2014

Communicated by Barry Lesht

*Index words:*
Stable isotopes
Great Lakes
Evaporation
Oxygen-18
Deuterium
Hydrology

ABSTRACT

We investigate the physical limnology of the Laurentian Great Lakes of North America using a new dataset of $^{18}O/^{16}O$ and $^{2}H/^{1}H$ ratios from over 500 water samples collected at multiple depths from 75 stations during spring and summer of 2007. $\delta^{18}O$ and $\delta^{2}H$ values of each lake plot in distinct clusters along a trend parallel to, but offset from, the Global Meteoric Water Line, reflecting the combined effects of evaporative enrichment and the addition of precipitation and runoff along the chain lake system. We apply our new dataset to a stable-isotope-based evaporation model that explicitly incorporates downwind lake effects, including humidity build-up and changes to the isotope composition of atmospheric vapor. Our evaporation estimates are consistent with previous mass transfer results for Michigan, Huron, Ontario and Erie, but not for Superior, which has a much longer residence time. Calculated evaporation from Superior is ~300 mm per year, less than previous estimates of ~500 mm per year, likely arising from integration of the 'isotopic memory' of lower evaporation rates under cooler climatic conditions with greater ice-cover than the present. Uncertainties in the estimates from the stable-isotope-based model are comparable to mass transfer results, offering an independent technique for evaluating evaporation fluxes.



## Introduction

The Laurentian Great Lakes are precious resources for both humans and nature. The chain lake system provides hydroelectric power, commercial and recreational fisheries, a shipping corridor to the Atlantic Ocean, and freshwater resources for agriculture, manufacturing and domestic uses, especially within the densely populated lower basin. About 10% (35 million) of the U.S. population and 25% (8 million) of the Canadian population live within the Great Lakes Basin, with the eight Great Lakes states and two provinces generating a quarter of North America's gross domestic product. As of 2014, Lakes Superior, Michigan and Huron are within a 15-year negative lake-level anomaly, the longest since records began in 1860 (Fig. 1). Changes in lake levels are driven by sustained imbalances between inputs (direct precipitation, river inflows) and losses (evaporation, river outflows) that change the volume of water retained in each Great Lake. Despite the impacts of lake-level fluctuations on lakeshore wetlands and a multi-billion dollar shipping industry, the response of regional precipitation fluxes and magnitude of changes in Great Lake evaporation under a warmer climate remain largely unknown with global climate models producing inconsistent projections of net water budgets (i.e., precipitation minus evapotranspiration; Angel and Kunkel, 2010; Hayhoe et al., 2010; Kutzbach et al., 2005). Our work uses an alternative approach based on assessment of variations in the relative abundances of the naturally occurring stable isotopes of oxygen ($^{18}O$) and hydrogen ($^{2}H$) embedded in the 'heavy' water isotopologues ($^{1}H^{1}H^{18}O$ and $^{1}H^{2}H^{16}O$) to provide residence-time-integrated estimates of net evaporation losses from each of the five North American Great Lakes.

Variability in the relative abundances of $^{18}O$ and $^{2}H$ in water, measured as $^{18}O/^{16}O$ and $^{2}H/^{1}H$ ratios, and expressed conventionally as $\delta^{18}O$ and $\delta^{2}H$ values (see below), can yield valuable insight into evaporation and mixing in hydrological systems. Evaporation can be assessed from increases in $\delta^{18}O$ and $\delta^{2}H$, reflecting enrichment of $^{1}H^{1}H^{18}O$ and $^{1}H^{2}H^{16}O$ in the liquid phase because of preferential loss of more volatile 'light' water molecules ($^{1}H^{1}H^{16}O$), while $\delta^{18}O$ and $\delta^{2}H$ values also serve as conservative tracers of mixing between waters having differing isotopic compositions. Previous stable isotope investigations of large lakes and inland seas have assessed evaporative losses (Lake Titicaca — Zuber, 1983; Mediterranean Sea — Gat et al., 1996; Lake Biwa — Taniguchi et al., 2000; Lake Edward — Russell and Johnson, 2006; Lake Okanagan — Wassenaar et al., 2011), intra-lake water mass mixing (Lake Chad — Fontes et al. 1970), the influence of past climates on lakes with long residence times (Lake Tanganyika — Craig, 1975; Lake Baikal — Seal and Shanks, 1998), mixing within a stratified water column (Lake Malawi — Gonfiantini et al., 1979), groundwater interactions (Lake Nasser — Aly et al., 1993; Lake Garda — Longinelli et al., 2008; Aral

* Corresponding author at: Department of Earth and Planetary Sciences, Northrop Hall, 1 University of New Mexico, Albuquerque, NM 87131, USA Tel.: +1 505 377 8368.
*E-mail address:* jasechko@unm.edu (S. Jasechko).

http://dx.doi.org/10.1016/j.jglr.2014.02.020
0380-1330/

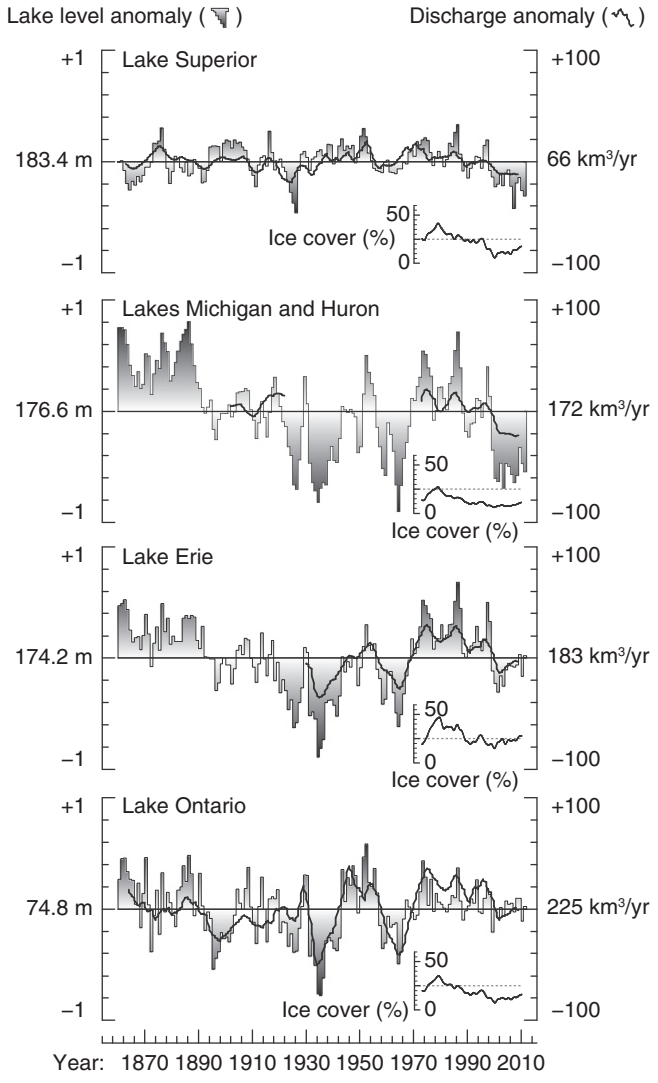


**Fig. 1.** Changes to Great Lake surface elevations (shaded bars) and liquid outflows (black line) from 1860 to present. Data plotted are relative to long-term mean lake level (m.a.s.l., left axis) and discharge ($km^3$/year, right axis). Annual average ice cover from for each Great Lake from 1973 to present is plotted as an inset (data from Wang et al., 2012). The upper Great Lakes (Superior, Michigan, Huron) are currently within the most prolonged negative lake level anomaly (15 years) since records began over a century ago.

Sea — Oberhänsli et al., 2009), lake outflows in downstream rivers (Lake Tahoe — McKenna et al., 1992; Tonlé Sap — Kabeya et al., 2008), transpiration losses (Okavango Swamp — Dinçer et al., 1978) and atmospheric moisture sources (Lac Léman — Fontes and Gonfiantini, 1970; North American Great Lakes — Gat et al., 1994; Machavaram and Krishnamurthy, 1995; Pyramid Lake — Benson and White, 1994; Lake Turkana — Ricketts and Johnson, 1996). Great Lakes evaporation has been estimated in previous studies using a combination of satellite (Lofgren and Zhu, 2000), eddy covariance (Blanken et al., 2011; Spence et al., 2011), energy balance (Croley, 1989; Croley and Assel, 1994; Morton, 1967) and mass balance techniques (Derecki, 1981; Hanrahan et al., 2010); but, until now, there has been no stable-isotope-based assessment of evaporation losses from each Great Lake.

*Study area*

The North American Great Lakes are located in the east-central part of the continent (Fig. 2). The set of five lakes cover less than 1% of the North American landmass but contain over 80% of the continent's fresh surface water. The Great Lakes drain 2500 km from Lake Superior to the St. Lawrence Seaway with an overall average residence time of 55 years (Table 1). Each Great Lake covers 25 to 40% of its own catchment area, a significantly higher proportion than the global average value of ~10% for lakes larger than 1000 $km^2$ (Jasechko et al., 2013).

Mean annual surface air temperatures range from +1 °C in the northern Lake Superior basin to +10 °C in the southern Michigan and Erie basins. Mean monthly temperatures within the Great Lakes Basin range from lows of −15 °C (north) to −2 °C (south) in February, up to +15 °C (north) to +22 °C (south) in August. Evaporation over the lakes is highly seasonal, with roughly 90% of annual evaporation occurring between September and February (Croley, 1989; Spence et al., 2011). In summer, evaporation over the lakes is near-zero due to the predominance of warm and humid air masses sourced from the Gulf of Mexico, creating stable atmospheric conditions (Magnuson et al., 1997; Rasmusen, 1968). However, in winter, the polar jet stream establishes in the southern portion of the catchment, permitting cool and dry air masses to enter the region from the northwest. As cold air masses advect over the Great Lakes, the air at the boundary layer warms by contact with comparatively warm Great Lake waters (+1 to +12 °C through fall and winter). Average winter evaporation rates increase to over 4 mm per day – more than twice the annual average rate – in response to cold, dry air and generally windier conditions over the lakes. Subsequent re-precipitation of evaporated moisture on comparatively cool downwind land produces the lake-effect snow belts along the leeward shores of the Great Lakes (Eichenlaub, 1970). The distinct signature of this phenomenon has been captured in several stable isotope investigations in the Great Lakes Basin (Bowen et al., 2012; Gat et al., 1994; Machavaram and Krishnamurthy, 1995) and elsewhere (e.g., Brock et al., 2009).

Spring and late winter evaporation fluxes are limited by the development of ice cover over the Great Lakes, which reaches a maximum in February or March (Wang et al., 2012). Ice cover varies in extent between years and amongst lakes. Average maximum ice cover decreases from Lake Erie (85%) to Superior and Huron (60%) to Michigan (40%) to Ontario (25%) (Assel et al., 2003; Bai et al., 2012). Annual mean ice cover has decreased since 1970 at a rate between 1.3% (Erie) and 2.3% (Ontario) per year (Fig. 1; Wang et al., 2012), plausibly related to observed increases in regional atmospheric temperatures (Bolsenga and Norton, 1993). Here, we investigate the hydrology and climatology of the five North American Great Lakes using measurements of stable oxygen and hydrogen isotope ratios in lake and catchment waters.

## Methods

Water samples from each of the five Great Lakes were collected during two cruises in the spring (31 March–18 April) and summer (1–24 August) of 2007 to assess both spatial and temporal variability in isotope compositions. In total, 514 samples were collected near the surface, at intermediate depth, and within 10 m of the bottom from 75 offshore sampling stations distributed amongst the Great Lakes (Fig. 2).

The $^{18}O/^{16}O$ and $^{2}H/^{1}H$ ratios of the water samples were determined by a Delta V Advantage isotope-ratio mass spectrometer on $CO_2$ and $H_2$ gas prepared using standard techniques (Epstein and Mayeda, 1953; Morrison et al., 2001). Results are expressed as $\delta^{18}O$ and $\delta^{2}H$ values, representing deviation in per mil (‰) in the relative abundances of $^{18}O$ or $^{2}H$ with respect to V-SMOW (Vienna Standard Mean Ocean Water) such that $\delta^{18}O_{sample}$ or $\delta^{2}H_{sample} = [(R_{sample} / R_{V\text{-}SMOW}) - 1] \cdot 1000$, where $R$ is the respective $^{18}O/^{16}O$ or $^{2}H/^{1}H$ ratio in sample and V-SMOW. Results are reported on the V-SMOW scale normalized to respective values of −55.5‰ and −428.0‰ for Standard Light Antarctic Precipitation (Coplen, 1996), accurate to within ±0.08‰ for $\delta^{18}O$ and ±0.5‰ for $\delta^{2}H$ (±2 standard deviations of repeat analyses).

The distribution of stable hydrogen and oxygen isotopes in global precipitation is characterized by the fundamental linear relation between $\delta^{2}H$ and $\delta^{18}O$ of amount-weighted mean annual precipitation at stations world-wide, well-described by the Global Meteoric Water Line

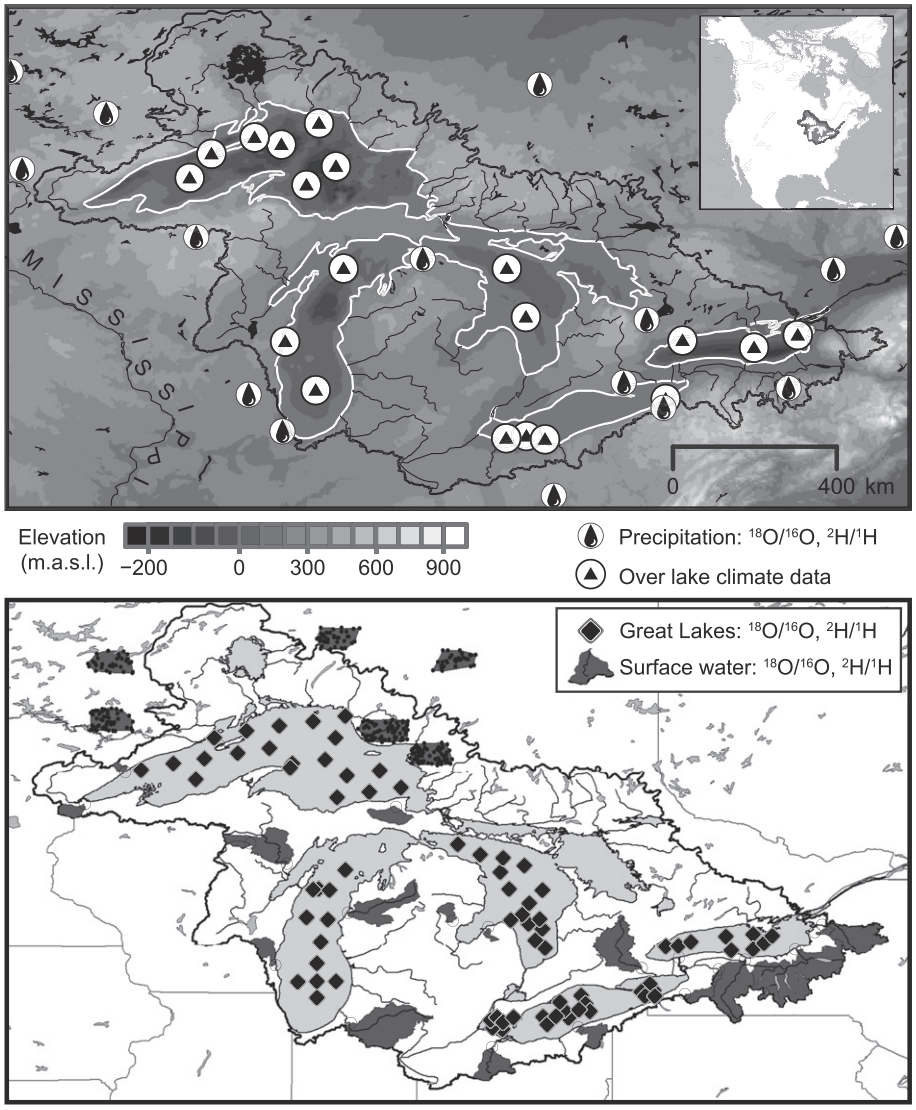


**Fig. 2.** Top panel gives locations of over-lake monitoring stations (triangles) and collection stations for $^{18}O/^{16}O$ and $^{2}H/^{1}H$ ratios in precipitation (water droplets) are shown with topography and bathymetry. Bottom panel gives locations of stations where Great Lakes waters were sampled at depth (diamonds) and surface water sampling stations in the Great Lakes catchment (sampled catchment marked in gray) are shown.

of Craig (1961) (GMWL: $\delta^2H = 8\ \delta^{18}O + 10$). Deviations from the GMWL reference line are indicated by the deuterium-excess parameter (*d-excess* $= \delta^2H - 8\ \delta^{18}O$), where *d-excess*$_{GMWL} = +10‰$ (Dansgaard, 1964).

Stable oxygen and hydrogen isotopic compositions of precipitation for 20 stations in the Great Lakes vicinity (Fig. 2A; Table 2) were obtained from the U.S. and Canadian Network(s) for Isotopes in Precipitation (Birks and Edwards, 2009; Birks and Gibson, 2009; Welker, 2000) and the International Atomic Energy Agency (Araguás-Araguás et al., 2000) databases. Isotope data for 20 river stations collected at one- to eight-month intervals were obtained from the United States Geological Survey (Kendall and Coplen, 2001) and the Grand River Conservation Authority (Fig. 2B, Table 3). This river dataset covers between 1% (Huron) and 40% (Ontario) of each Great Lake catchment. Isotopic data for 312 small (<100 km$^2$) lakes in the Lake Superior catchment have also been compiled from acid sensitivity surveys (Fig. 2; unpublished data from Environment Canada/Alberta Innovates - Technology Futures) and plot along a regression of $\delta^2H = 5.14\ \delta^{18}O - 25.5$; $R^2 = 0.852$.

**Table 1**
Physical characteristics of the North American Great Lakes.

| Lake | Lake area (km$^2$) | Catchment area (km$^2$) | Lake area ÷ catchment area (%) | Level (m.a.s.l.) | Residence time[a] (years) | Volume (km$^3$) | Depth (m) | |
|---|---|---|---|---|---|---|---|---|
| | | | | | | | Avg. | Max. |
| Superior | 82,000 | 210,000 | 39 | 183.4 | 173 | 12,000 | 147 | 405 |
| Huron | 60,000 | 193,000 | 31 | 176.5 | 21 | 3500 | 59 | 281 |
| Michigan | 58,000 | 176,000 | 33 | 176.5 | 62 | 4900 | 85 | 229 |
| Erie | 26,000 | 85,000 | 31 | 174.1 | 2.7 | 480 | 19 | 64 |
| Ontario | 19,000 | 80,000 | 24 | 74.8 | 7.5 | 1600 | 87 | 244 |

[a] Residence times from Quinn (1992).

**Table 2**
Monitoring stations for $^{18}O/^{16}O$ and $^{2}H/^{1}H$ ratios of precipitation in the North American Great Lakes region.

| Station | Network | Lat. (°) | Lon. (°) | Alt. (m.a.s.l.) | Years active | $\delta^{18}O$[a] (‰) | $\delta^{2}H$[a] (‰) | *d-Excess* (‰) | n | Meteoric water line |
|---|---|---|---|---|---|---|---|---|---|---|
| Atikokan | IAEA | 48.75 | −91.62 | 393 | 1975–1982 | −12.61 | −91.5 | 9.4 | 75 | $\delta^2H = 7.84 \times \delta^{18}O + 7.5$ |
| Aurora | USNIP | 42.73 | −76.66 | 249 | 1989–1994 | −8.12 | −57.3 | 7.7 | 27 | $\delta^2H = 7.65 \times \delta^{18}O + 10.5$ |
| Bonner Lake | CNIP | 49.38 | −82.12 | 245 | 1993–2003 | −13.82 | −100.7 | 9.9 | 121 | $\delta^2H = 7.70 \times \delta^{18}O + 5.1$ |
| Caldwell | USNIP | 39.79 | −81.53 | 276 | 1989–1990 | | −40.4 | | 30 | |
| Chapais | CNIP | 49.82 | −74.97 | 382 | 1993–2003 | −13.40 | −97.3 | 9.9 | 122 | $\delta^2H = 7.80 \times \delta^{18}O + 8.5$ |
| Chautauqua | USNIP | 42.30 | −79.40 | 488 | 1989–1993 | −8.36 | −55.5 | 11.4 | 27 | $\delta^2H = 7.05 \times \delta^{18}O + 4.3$ |
| Chicago | IAEA | 41.78 | −87.75 | 189 | 1960–1979 | −6.18 | −44.7 | 4.7 | 170 | $\delta^2H = 6.98 \times \delta^{18}O + 0.1$ |
| Coshocton | IAEA | 40.37 | −81.80 | 344 | 1966–1971 | −7.41 | −46.6 | 12.7 | 64 | $\delta^2H = 7.51 \times \delta^{18}O + 8.8$ |
| Douglas Lake | USNIP | 45.56 | −84.68 | 238 | 1989–1990 | −10.27 | | | 23 | |
| Egbert | CNIP | 44.23 | −79.77 | 224 | 1993–2003 | −10.35 | −72.8 | 10.0 | 65 | $\delta^2H = 6.86 \times \delta^{18}O - 2.6$ |
| Exp. Lakes | CNIP | 49.67 | −93.72 | 369 | 1993–2003 | −12.33 | −90.3 | 8.3 | 123 | $\delta^2H = 7.75 \times \delta^{18}O + 5.0$ |
| Gimli | IAEA | 50.62 | −96.98 | 223 | 1975–1982 | −14.21 | −103.7 | 10.0 | 73 | $\delta^2H = 7.65 \times \delta^{18}O + 3.0$ |
| Lake Geneva | USNIP | 42.58 | −88.50 | 288 | 1989–1993 | −7.51 | −52.4 | 7.7 | 43 | $\delta^2H = 7.20 \times \delta^{18}O - 0.1$ |
| Marcell | USNIP | 47.53 | −93.47 | 431 | 1989–1994 | −11.17 | −89.1 | 0.3 | 61 | $\delta^2H = 8.11 \times \delta^{18}O + 11.8$ |
| Ottawa | IAEA | 45.32 | −75.67 | 114 | 1953–2007 | −10.97 | −75.2 | 12.6 | 556 | $\delta^2H = 7.57 \times \delta^{18}O + 7.1$ |
| Penn State | USNIP | 40.79 | −77.95 | 393 | 1989–1989 | | −40.4 | | 26 | |
| Simcoe | IAEA | 42.85 | −80.27 | 240 | 1975–1982 | −9.27 | −62.2 | 12.0 | 78 | $\delta^2H = 7.80 \times \delta^{18}O + 9.4$ |
| Ste. Agathe | IAEA | 46.05 | −74.28 | 395 | 1975–1982 | −12.55 | −87.8 | 12.6 | 80 | $\delta^2H = 7.75 \times \delta^{18}O + 10.0$ |
| The Pas | IAEA | 53.97 | −101.1 | 272 | 1975–1982 | −16.55 | −125.8 | 6.6 | 70 | $\delta^2H = 7.57 \times \delta^{18}O - 0.4$ |
| Trout Lake | USNIP | 46.05 | −89.65 | 501 | 1989–1991 | −9.06 | −67.3 | 5.2 | 31 | $\delta^2H = 8.12 \times \delta^{18}O + 14.9$ |

[a] $\delta^{18}O$ and $\delta^{2}H$ values presented here are flux-weighted by Eq. (5).

Physical hydrologic data for the Great Lakes were derived from the Great Lakes Environmental Research Laboratory (T. Hunter, pers. comm.). Hydroclimate data were obtained from 19 monitoring buoys distributed amongst the five Great Lakes (National Data Buoy Center; Fig. 2A) and from gridded meteorological datasets (Mesinger et al., 2005; New et al., 2002).

*Isotope results*

As shown in Fig. 3 (and tabulated in Electronic Supplemental Material (ESM) Table S1), the data obtained from the two sampling campaigns plot in a linear array spanning narrow ranges of isotopic composition (~24‰ for $\delta^{2}H$; ~3‰ for $\delta^{18}O$). Clusters of data from Michigan and Superior anchor the upper and lower ends of the trend, respectively, while data from Huron, Erie and Ontario plot in intermediate positions. Bivariate regression through the entire dataset yields a best-fit 'Great Lakes Water Line' (GLWL: $\delta^2H = 8.0\ \delta^{18}O + 3.2$) that is parallel to, but offset below, the GMWL. The shift to lower *d-excess* in each lake is the net effect of open-water evaporation, which enriches the isotopic composition of the remaining water along relatively shallow trajectories (slope < 8) below the GMWL, variably compensated by the addition of direct precipitation and runoff, which tends to draw the isotopic composition of each lake back towards the GMWL (Fig. 4A). The distribution of the data clusters along the GLWL can be reconciled qualitatively with the differing hydrologic settings of the individual lakes within the Great Lakes system. The pronounced displacement between Michigan and Superior, for example, is largely attributable to latitude-dependent differences in the isotopic composition of precipitation and runoff in these two headwater catchments, whereas the positions of the other three lakes reflect varying influence of 'pre-evolved' contributions from upstream lakes, in addition to local evaporation, precipitation and runoff.

**Table 3**
Monitoring stations for $^{18}O/^{16}O$ and $^{2}H/^{1}H$ ratios of river water in the North American Great Lakes catchment.

| River | Lake catchment | Station number | Lat. (°) | Lon. (°) | Alt. (m.a.s.l.) | Catchment ($km^2$) | $\delta^{18}O$[a] (‰) | $\delta^{2}H$[a] (‰) | *d-Excess* (‰) | n | Discharge ($km^3$/year) |
|---|---|---|---|---|---|---|---|---|---|---|---|
| Baptism R. | Superior | 4014500 | 47.34 | −91.20 | 187 | 360 | −10.14 | −73.3 | 7.8 | 10 | 0.11 |
| Nemadji R. | Superior | 4024430 | 46.63 | −92.09 | 191 | 1090 | −12.03 | −84.3 | 11.9 | 11 | 0.39 |
| Tahquamenon R. | Superior | 4045500 | 46.58 | −85.27 | 212 | 2050 | −12.31 | −85.2 | 13.2 | 10 | 0.89 |
| Washington Ck. | Superior | 4001000 | 47.92 | −89.15 | 184 | 30 | −12.42 | −87.2 | 12.2 | 11 | 0.01 |
| Pigeon R. | Huron | 4159010 | 43.94 | −83.24 | 183 | 320 | −10.81 | −73.9 | 12.5 | 10 | 0.26 |
| Rifle R. | Huron | 4142000 | 44.07 | −84.02 | 198 | 830 | −11.13 | −77.7 | 11.3 | 9 | 0.61 |
| Manistee R. | Michigan | 4126520 | 44.25 | −86.32 | 184 | 5180 | −10.83 | −73.9 | 12.7 | 16 | 2.6 |
| Menominee R. | Michigan | 4067500 | 45.32 | −87.66 | 192 | 10180 | −10.80 | −76.3 | 10.1 | 8 | 3.2 |
| Milwaukee R. | Michigan | 4087000 | 43.10 | −87.91 | 185 | 1800 | −10.24 | −69.8 | 12.1 | 9 | 0.95 |
| Popple R. | Michigan | 4063700 | 45.76 | −88.46 | 429 | 360 | −10.77 | −75.7 | 10.5 | 11 | 0.08 |
| St. Joseph R. | Michigan | 4101500 | 41.83 | −86.26 | 193 | 9500 | −7.98 | −52.9 | 10.9 | 16 | 3.9 |
| Cattaraugus Ck. | Erie | 4213500 | 42.46 | −78.94 | 225 | 1130 | −10.62 | −70.6 | 14.4 | 11 | 0.9 |
| Grand R. (Canada) | Erie | At York | 43.02 | −79.89 | 190 | 6500 | −10.70 | −74.0 | 11.5 | 72 | 1.8 |
| Grand R. (U.S.A.) | Erie | 4212200 | 41.74 | −81.27 | 177 | 1820 | −9.25 | −60.2 | 13.9 | 7 | 1.4 |
| Sandusky R. | Erie | 4198000 | 41.31 | −83.16 | 191 | 3240 | −8.01 | −50.7 | 13.3 | 12 | 0.92 |
| Black R. | Ontario | 4260500 | 43.99 | −75.93 | 114 | 4850 | −11.12 | −75.7 | 13.3 | 17 | 3.0 |
| Genesee R. | Ontario | 4232006 | 43.22 | −77.62 | 105 | 6360 | −8.95 | −60.8 | 10.7 | 4 | 1.9 |
| Oswego R. | Ontario | 4249000 | 43.45 | −76.51 | 75 | 13210 | −9.46 | −65.7 | 9.9 | 11 | 4.8 |
| Sandy Ck. | Ontario | 4250750 | 43.81 | −76.08 | 160 | 330 | −11.51 | −77.0 | 15.1 | 17 | 0.21 |
| Tonawanda Ck. | Ontario | 4217000 | 43.00 | −78.19 | 267 | 440 | −11.04 | −74.2 | 14.2 | 7 | 0.18 |

[a] $\delta^{18}O$ and $\delta^{2}H$ values presented here are discharge-weighted by Eq. (6).

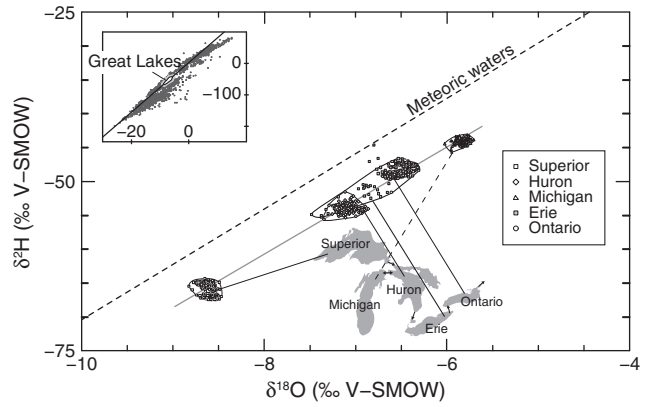


**Fig. 3.** Isotopic composition of the waters of the five North American Great Lakes. The Global Meteoric Water Line (Craig, 1961) is shown for reference (GMWL: $\delta^2H = 8\ \delta^{18}O + 10$). The best-fit Great Lakes Water Line (GLWL) is described by $\delta^2H = 8.0\ \delta^{18}O + 3.2$ ($R^2 = 0.98$). Data from each lake is encircled and connected to a corresponding Great Lake (note three suspect points for Lake Erie and one from Lake Ontario are not encircled). Inset in upper left shows $\delta^{18}O$ and $\delta^2H$ values of global lakes (Jasechko et al., 2013) to provide context.

Closer examination of the isotopic data reveals detectable, though minor, differences in the degree of spatial and temporal variability amongst the lakes (Table 4; Fig. 5). The water mass of Lake Michigan is the most homogeneous, with nearly negligible variability in isotopic composition both spatially and between the sampling campaigns, and an average *d-excess* of +2.5‰, slightly below the GLWL *d-excess* of +3.2‰. Lake Ontario waters also appear to be well-mixed, with an overall average *d-excess* of +3.5‰, close to that of the GLWL. In contrast, the waters of Superior and Huron both exhibit slightly lower average $\delta^2H$ and *d-excess* in spring than in summer, likely reflecting incomplete mixing of early-season runoff. The overall average isotope composition of Lake Superior waters lies directly upon the GLWL (*d-excess* = +3.2‰), while Huron waters are offset slightly below this reference line (average *d-excess* = +2.6‰). Lake Erie shows the largest range of $\delta^{18}O$ and $\delta^2H$ values of all the Great Lakes, increasing eastward from the Detroit River (inflow) to the Niagara River (outflow), and displays the highest average *d-excess* of +3.8‰. The systematic spatial variability in this shallow water body is likely attributable to a combination of increasing cumulative evaporative losses to the east and incomplete longitudinal mixing during fall and spring turnover. Isotopic stratification did not develop in any of the lakes during 2007 (Fig. 5), consistent with low rates of summer evaporation (Croley, 1989; Spence et al., 2011).

The isotopic data obtained for each of the Great Lakes can be used to quantify evaporation fluxes using a linear resistance model developed to estimate the isotopic composition of evaporating moisture (Craig and Gordon, 1965). The following calculation section outlines steps taken to calculate an isotope-based evaporation flux for each of the five Great Lakes.

### *Calculation*

An open-water reservoir can be described in terms of inputs, outputs and changes to storage:

$$\frac{dV}{dt} = I - O - E \tag{1}$$

where each successive term represents the rate of change in storage $\left(\frac{dV}{dt}\right)$, the sum of all fluxes entering the lake ($I$), surface outflow from the lake ($O$) and evaporation from the lake surface ($E$). Note that groundwater recharge and discharge to the Great Lakes is neglected in this mass balance given that the highest estimates of groundwater exchange are <10% of over-lake precipitation and catchment runoff (Neff and Nicholas, 2005).

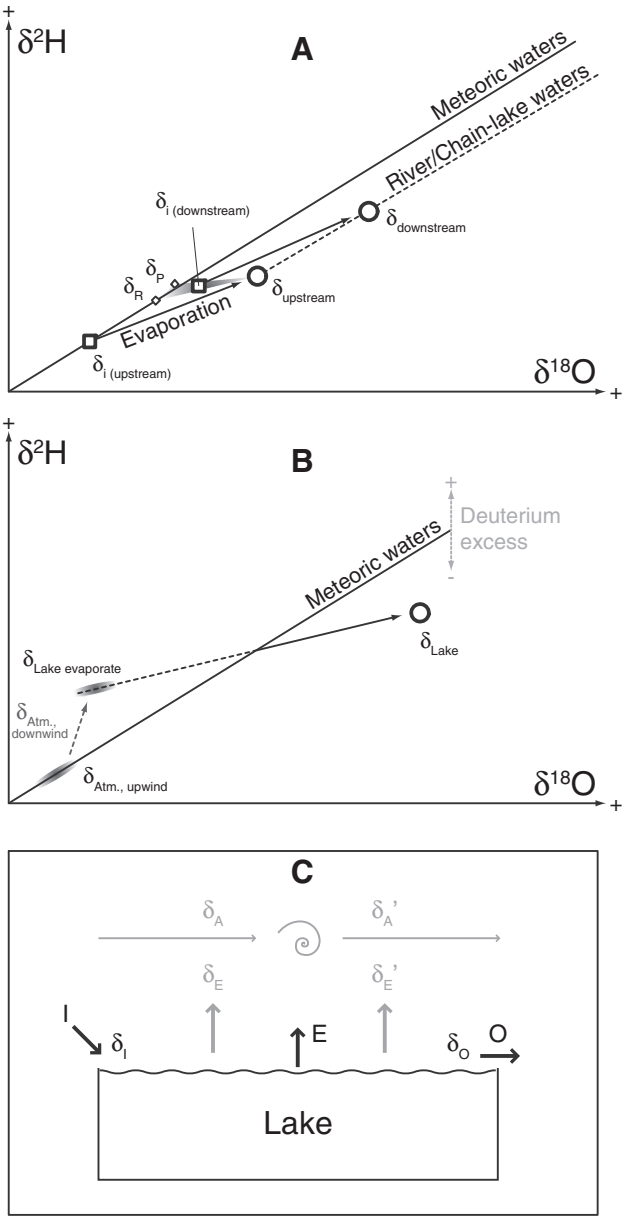


**Fig. 4.** (A) Schematic for the $\delta^{18}O$ and $\delta^2H$ values of an evaporating chain-lake or river system. Headwater inputs ($\delta_{i(upstream)}$), downstream precipitation ($\delta_P$) and catchment runoff ($\delta_R$) plot near to the Global Meteoric Water Line, whereas the isotopic composition of upstream and downstream lakes (circles, $\delta_{upstream}$ and $\delta_{downstream}$) plots along a line that is parallel to and offset from the meteoric water line, reconciled by a balance of evaporation losses and meteoric inputs of water. The isotopic composition of downstream inputs ($\delta_{i(downstream)}$) is calculated by weighting $\delta_P$, $\delta_R$ and $\delta_{upstream}$ to the respective fluxes of each input component (grayscale triangle). (B) Schematic showing the impact of lake evaporate on the isotopic composition of the downwind atmosphere overlying a lake surface. (C) Schematic showing an isotope mass balance for a large lake that influences its own regional climate. Water fluxes including inputs ($I$; precipitation, runoff and upstream inflows), evaporate ($E$) and outflow ($O$) are represented by thick black arrows. The isotopic compositions of each flux and reservoir (e.g. atmosphere: $\delta_A$) are represented by $\delta$ symbols. Primed values for the atmosphere ($\delta_A'$) and evaporate ($\delta_E'$) denote downwind scenarios where upwind evaporate has influenced the isotopic composition of the downwind atmosphere.

Similarly, a stable isotope mass balance for a surface water reservoir can be expressed as (Gilath and Gonfiantini, 1983):

$$\delta_L \frac{dV}{dt} + V\frac{d\delta_L}{dt} = \delta_I I - \delta_O O - \delta_E E \tag{2}$$

**Table 4**
$\delta^{18}O$, $\delta^{2}H$ and *d-excess* mean values and one standard deviation (s.d.) of North American Great Lake waters (expressed in units of ‰).

| Lake | Sampling | n | $\delta^{2}H$ | 1 s.d. $\delta^{2}H$ | $\delta^{18}O$ | 1 s.d. $\delta^{18}O$ | *d-excess* | 1 s.d. *d-excess* |
|---|---|---|---|---|---|---|---|---|
| Superior | Spring | 80 | −66.3 | 0.8 | −8.60 | 0.06 | 2.5 | 1.0 |
| | Summer | 60 | −65.0 | 0.3 | −8.66 | 0.06 | 4.2 | 0.6 |
| | Average | | −65.8 | 0.9 | −8.62 | 0.07 | 3.2 | 1.2 |
| Huron | Spring | 60 | −54.4 | 0.4 | −7.05 | 0.10 | 2.1 | 0.7 |
| | Summer | 45 | −53.4 | 0.6 | −7.09 | 0.06 | 3.4 | 0.7 |
| | Average | | −53.9 | 0.7 | −7.06 | 0.09 | 2.6 | 1.0 |
| Michigan | Spring | 44 | −44.2 | 0.3 | −5.83 | 0.06 | 2.5 | 0.5 |
| | Summer | 36 | −44.2 | 0.6 | −5.84 | 0.07 | 2.5 | 0.6 |
| | Average | | −44.2 | 0.5 | −5.83 | 0.06 | 2.5 | 0.6 |
| Erie | Spring | 63 | −49.9 | 2.8 | −6.69 | 0.37 | 3.6 | 0.8 |
| | Summer | 63 | −48.7 | 1.6 | −6.60 | 0.15 | 4.1 | 1.1 |
| | Average | | −49.3 | 2.3 | −6.64 | 0.29 | 3.8 | 1.0 |
| Ontario | Spring | 36 | −49.1 | 0.2 | −6.62 | 0.04 | 3.8 | 0.4 |
| | Summer | 27 | −49.0 | 0.4 | −6.51 | 0.08 | 3.1 | 0.4 |
| | Average | | −49.1 | 0.3 | −6.57 | 0.08 | 3.5 | 0.5 |

where $\delta$ denotes the isotopic composition of the lake (subscript $L$) or water flux (inputs, $I$; outflows, $O$; evaporate $E$) described in Eq. (1). The Great Lakes are near steady-state both hydrologically and isotopically, as Great Lake volumes have not fluctuated more than 5% within the residence time of each lake since 1860 (Fig. 1); and the isotopic composition of each lake has not changed dramatically over the past 40 years (<2‰ change in $\delta^{2}H$ based on comparison with data from Brown, 1970). Combining Eqs. (1) and (2) and assuming outflowing water within a Great Lake's connecting channel is representative of the isotopic composition of the lake (i.e., $\delta_O = \delta_L$), we develop an

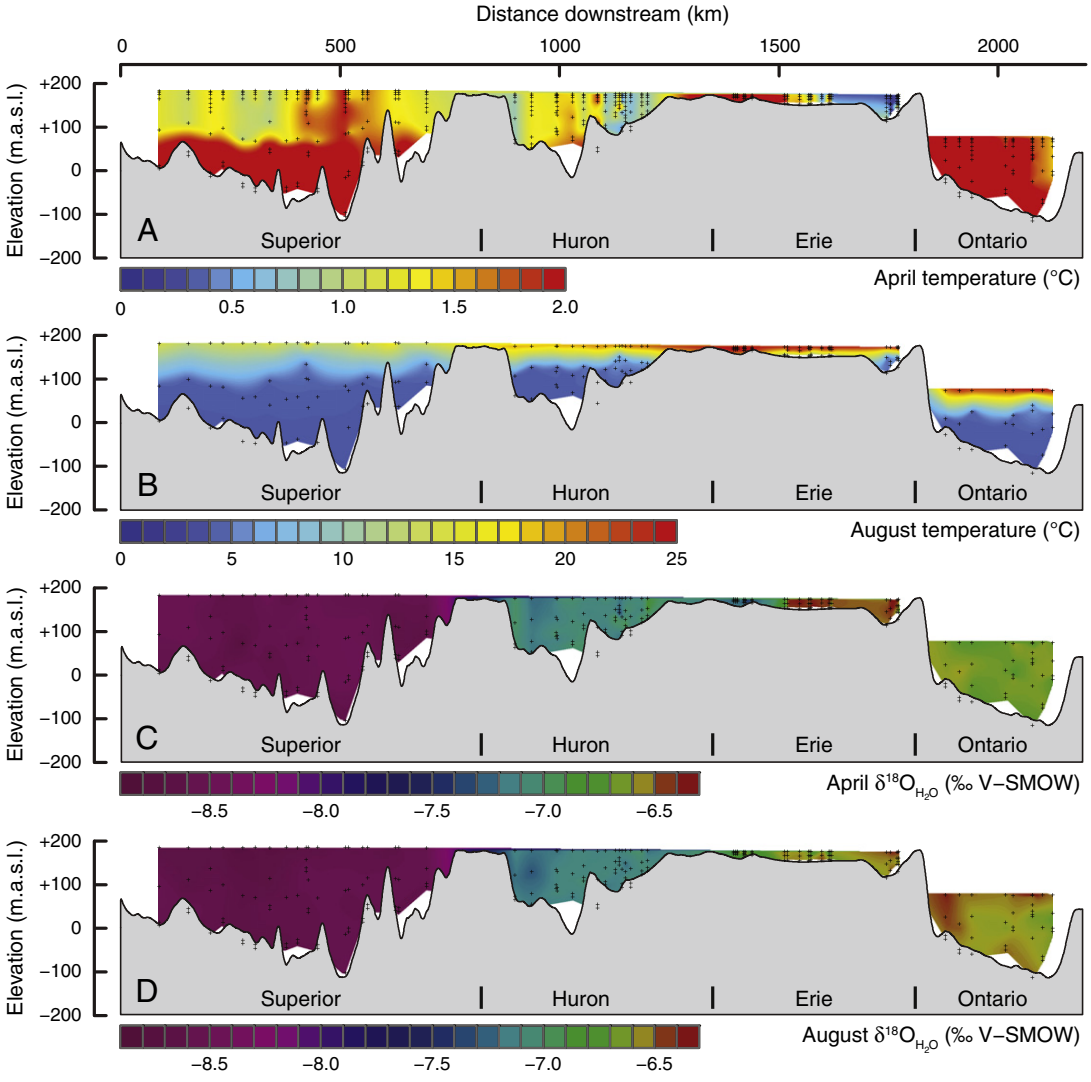


**Fig. 5.** Temperature and $\delta^{18}O$ profiles of Superior, Huron, Erie, and Ontario in April (A, C) and August (B, D) 2007.

expression for evaporation losses from an exorheic (open drainage) lake at steady state (Eq. (3)):

$$E = O \cdot \frac{\delta_I - \delta_L}{\delta_E - \delta_I}. \quad (3)$$

Eq. (3) is preferred instead of more common *E/I* ratios (e.g., Gibson and Edwards, 2002) because liquid outflows are far better constrained (±2% to ±10%) than precipitation and runoff (±40%; Neff and Nicholas, 2005) fluxes for the Great Lakes.

To calculate evaporation using Eq. (3) four input parameters are required: $O$, $\delta_L$, $\delta_I$ and $\delta_E$. Outflow ($O$) is well-constrained by gauge measurements at the outlets of each Great Lake (Fig. 1). The isotopic composition of each Great Lake ($\delta_L$) is investigated here, leaving only the isotopic composition of hydrologic inputs ($\delta_I$) and that of evaporate ($\delta_E$) to be evaluated.

Hydrologic inputs entering a lake ($I$, $\delta_I$) can be partitioned into three components: connecting channel inflows ($U$, $\delta_U$); direct over-lake precipitation ($P$, $\delta_P$); and catchment runoff ($R$, $\delta_R$; i.e., $I = U + P + R$). The isotopic composition of inputs to each Great Lake can be calculated by flux-weighting the isotopic composition of each input component (Eq. (4)).

$$\delta_I = \frac{U\delta_U + P\delta_P + R\delta_R}{U + P + R} \quad (4)$$

The isotopic composition of connecting channel inflows ($\delta_U$) has been derived from samples collected near the outlet of the nearest upstream Great Lake. Connecting channel fluxes ($U$) are obtained from river gauging data (Fig. 1). In the case of Lake Huron, chain-lake inflows enter from both Superior (St. Mary's River) and Michigan (Straits of Mackinac). Inflows from Superior are well-constrained by river gauging and fluxes at the Straits of Mackinac have been calculated previously (Chapra et al., 2009, Quinn, 1992). The isotopic composition of connecting channel inflows ($\delta_U$) does not include a seasonality component because of the multi-year residence times of all of the individual Great Lakes.

The isotopic composition of precipitation has been measured at 20 stations in the Great Lakes region (Fig. 2A, Table 2). For each station, the amount-weighted isotopic composition for each precipitation monitoring station ($\delta_{P(aw)}$) was calculated by weighting the isotopic composition of precipitation to monthly precipitation amount via Eq. (5):

$$\delta_{P(aw)} = \frac{\sum_{i=1}^{12} \delta_{P(i)} P_i}{\sum_{i=1}^{12} P_i} \quad (5)$$

where $\delta_{P(i)}$ represents the isotopic composition of precipitation integrated over month $i$ and $P_i$ is the amount of precipitation falling during month $i$.

Similar to precipitation, the isotopic composition of 20 rivers within the Great Lakes catchment was measured at one- to eight-month intervals between 1984 and 1987 (Kendall and Coplen, 2001). Corresponding monthly discharge data have been collected from the National Water Information System (waterdata.usgs.gov). A flow-weighted isotopic composition for each river monitoring station ($\delta_{R(fw)}$) was calculated following Eq. (6):

$$\delta_{R(fw)} = \frac{\sum_{i=1}^{12} \delta_{R(i)} R_i}{\sum_{i=1}^{12} R_i} \quad (6)$$

where $\delta_{R(i)}$ represents the isotopic composition of river water sampled during month $i$ and $R_i$ represents monthly average discharge. However, since the spatial distribution of precipitation ($\delta_{P(aw)}$) and river ($\delta_{R(fw)}$) sampling sites does not cover the entire Great Lakes catchment, gridded data were used.

To develop gridded data specific to the Great Lakes region, we first obtained monthly 10′ by 10′ global gridded estimates of the isotopic composition of precipitation (Bowen and Revenaugh, 2003; Bowen and Wilkinson, 2002) developed using stepwise regression of latitude and altitude with $\delta^{18}O$ and $\delta^2H$ in precipitation ($\delta_{P(BW)}$). Grid values for $\delta_{P(BW)}$ at each precipitation monitoring location and within each river catchment (Fig. 2B) were calculated and compared with measured values at 20 precipitation and 20 river stations. A cross-plot of $\delta_{P(BW)}$ gridded values and measured values at 20 precipitation and 20 river stations produced the regressions: $\delta^{18}O_{P(BW)} = 1.154 \cdot \delta^{18}O_{meas} + 1.16$ ($R^2 = 0.59$) and $\delta^2H_{P(BW)} = 1.215 \cdot \delta^2H_{meas} + 11.8$ ($R^2 = 0.66$). These regressions were applied to $\delta_{P(BW)}$ grids to develop a re-calibrated gridded dataset of $\delta^{18}O$ and $\delta^2H$ values of precipitation specifically for the Great Lakes region.

This new localized gridded dataset was used to calculate the isotopic composition of direct precipitation ($\delta_P$) and river inputs ($\delta_R$) for each Great Lake. An average of over-lake grids was used to calculate the isotope composition of direct precipitation falling on each Great Lake ($\delta_P$). Similarly, we used an average of localized grids on land within each Great Lake catchment to estimate $\delta_R$. Because a strong evaporative signal was not evident from the *d-excess* in any of the rivers sampled, we assume that catchment runoff in the Great Lakes basin has not been strongly affected by evaporation and that transpiration – which does not produce an isotope effect on waters under steady-state conditions – dominates total catchment evapotranspiration (Jasechko et al., 2013; Karim et al., 2008).

Lastly, we assess the isotopic composition of Great Lake evaporate ($\delta_E$) using the Craig and Gordon (1965) model:

$$\delta_E = \frac{(\delta_L - [\alpha_{l\text{-}v}{}^* - 1])/\alpha_{l\text{-}v}{}^* - h\delta_A - (C_k[1-h])}{1 - h + (C_k[1-h])} \quad (7)$$

where $\delta_L$ is the isotope composition of a Great Lake, $\alpha_{l\text{-}v}{}^*$ is a temperature-dependent equilibrium liquid–vapor isotopic fractionation factor, $h$ represents atmospheric relative humidity normalized to surface temperatures of each Great Lake, $\delta_A$ represents the isotopic composition of the overlying atmosphere and $C_k$ is a kinetic fractionation constant equal to 0.0172 ± 0.0035 for $\delta^{18}O$-based and 0.0118 ± 0.0043 for $\delta^2H$-based evaporation models, respectively (uncertainty in $C_k$ captures transitional zone between smooth and turbulent transport conditions, Fig. 6; see reviews of Gat, 1996 and Horita et al., 2008). To use Eq. (7) four input parameters are required: the isotopic composition of the lake ($\delta_L$, reported in this work), lake temperature ($T_L$), atmospheric relative humidity ($h$), and the isotopic composition of the atmosphere overlying each Great Lake ($\delta_A$).

First, to calculate the equilibrium liquid–vapor fractionation factors ($\alpha_{l\text{-}v}{}^*$) for $\delta^{18}O$ and $\delta^2H$, monthly average lake surface temperatures were collected from over-lake monitoring buoy records (National Data Buoy Center: www.ndbc.noaa.gov). Long-term monthly mean lake surface temperatures are entered into empirical formulae developed by Horita and Wesolowski (1994) to calculate the temperature-dependent $\alpha_{l\text{-}v}{}^*$ values.

Next, atmospheric relative humidity values were derived from near-surface gridded atmospheric datasets (New et al., 2002) and converted to specific humidity ($e$; Buck, 1981) using long-term mean monthly air temperatures ($T_A$; New et al., 2002). A new saturation vapor pressure was calculated applying monthly lake surface temperature data from monitoring buoys and was used to calculate a relative humidity normalized to lake surface temperatures ($h$).

Initial estimates of monthly $\delta_A$ values were calculated using an assumption of isotopic equilibrium between vapor and monthly precipitation (see Gibson et al., 2008). This equilibrium assumption appears to be valid at a global scale since $\delta^2H \div \delta^{18}O$ regressions of precipitation (Craig, 1961; Rozanski et al., 1993) follow a similar slope to equilibrium fractionation based on experimentally determined equilibrium liquid–vapor fractionation factors ($\alpha_{l\text{-}v}{}^*$; Horita and Wesolowski, 1994).

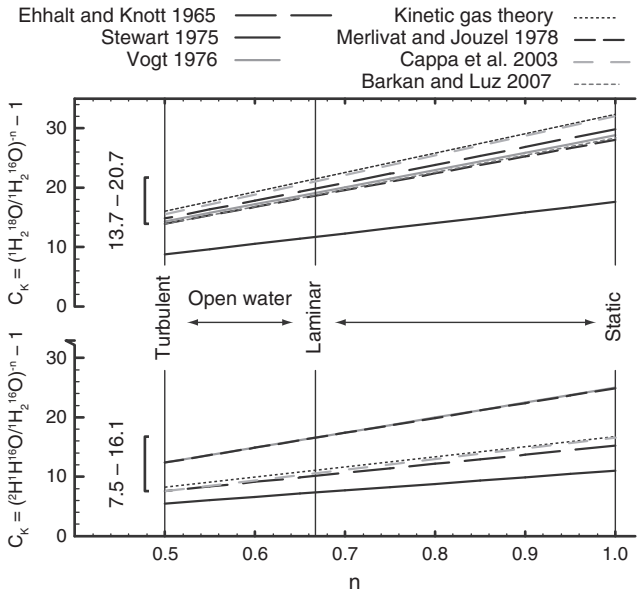


**Fig. 6.** Calculation of kinetic fractionation constants ($C_k$) for $\delta^{18}O$ (upper) and $\delta^2H$ (lower) for the liquid–vapor phase transition using diffusivity ratios from multiple sources compiled by Horita et al. (2008; data from Ehhalt and Knott, 1965; Stewart, 1975; Vogt, 1976; Merlivat and Jouzel, 1978; Cappa et al., 2003; Barkan and Luz, 2007). The term $n$ reflects evaporation conditions and ranges from fully turbulent open-water evaporation ($n = 1/2$), to laminar open-water evaporation (smooth conditions, $n = 2/3$) to static transport (i.e., soil evaporation, $n \approx 1$). Open water evaporation is represented by $0.5 < n < 0.67$, producing kinetic fractionation constants of: $13.7 < C_k(\delta^{18}O) < 20.7$ and $7.5 < C_k(\delta^2H) < 16.1$ (Stewart, 1975; data not included).

Monthly average over-lake air temperatures (New et al., 2002) were used to calculate atmospheric liquid–vapor fractionation factors (Horita and Wesolowski, 1994). We estimate $\delta_A$ over each of the Great Lakes by applying monthly atmospheric equilibrium fractionation factors to localized grids of the isotope composition of precipitation.

All of the above parameters (i.e., $\delta_A$, air and lake temperature, specific humidity) have been weighted at a monthly time-step to estimates of monthly evaporation percentage from the Great Lakes Environmental Research Laboratory (GLERL; T. Hunter, personal communication) as proposed by Gibson et al. (2008) to develop representative annual values. Calculation inputs are shown in Tables 4 and 5.

The processes of moisture recycling and lake effects on the atmosphere have been established as important regional phenomena in the North American Great Lakes catchment (Eichenlaub, 1970). Evaporation from Great Lakes adds considerable moisture to the overlying atmosphere as air masses advect over the lakes and deposit lake-effect precipitation on the leeward shores ('snow belts'). Kinetic isotope effects during evaporation influence the isotopic composition of the atmosphere by increasing the *d-excess* values of moisture downwind of the Great Lakes (Gat et al., 1994; Machavaram and Krishnamurthy, 1995; Bowen et al., 2012; see schematic in Fig. 6b). This is best shown by lower *d-excess* of precipitation stations upwind of the Great Lakes (e.g., Chicago, *d-excess* = +4.7‰; Experimental Lakes Area (northwestern Ontario), *d-excess* = +8.3‰; Marcell Experimental Forest (Minnesota), *d-excess* = 0.3‰) relative to stations on leeward shores (e.g., Chautauqua (New York), *d-excess* = +11.4‰; Egbert, *d-excess* = +10.0‰; Simcoe (southern Ontario), *d-excess* = +12.0‰; Table 2). We propose a modified version of the Craig–Gordon evaporation model (Craig and Gordon, 1965) that simultaneously uses both $\delta^{18}O$ and $\delta^2H$ values to better constrain evaporative losses over large lakes.

First, Eq. (7) was applied to develop a first estimate of the isotope composition of evaporate ($\delta_{E(\text{upwind})}$). Next, this first estimate was mixed incrementally with our equilibrium-based isotope composition of atmospheric vapor ($\delta_A$; Table 5) to produce a new "downwind" estimate for the isotope composition of atmospheric moisture value over each Great Lake that has incorporated a certain amount of evaporate ($\delta_{A'}$).

$$\delta_{A'} = (1-x)\delta_A + x\delta_E \tag{8}$$

$$\delta_{E'} = \frac{(\delta_L - [\alpha_{l\text{-}v} * -1])/\alpha_{l\text{-}v} * h\delta_{A'} - (C_k[1-h])}{1-h+(C_k[1-h])} \tag{9}$$

where $x$ represents the percentage of evaporated moisture required to produce unity between the $\delta^{18}O$- and $\delta^2H$-based evaporation estimates, consistent with conservation of mass and isotopes (following Yi et al., 2008). In effect, this causes $\delta_{A'}$ values to trend to higher deuterium excess values downwind (Fig. 4B). The same mixing scheme is applied to specific humidity and temperature by incrementally adding saturated air with a temperature averaged between the lake surface and the upwind atmosphere. This mixing model is iterated until evaporation outputs for both $\delta^{18}O$ and $\delta^2H$ converge upon a matching value for evaporation over each Great Lake (see schematic in Fig. 4C).

Each of the calculation parameters contains uncertainty (Tables 5 and 6), which was assessed through a Monte-Carlo analysis. A normal distribution about the mean values of each calculation input was created, with the uncertainty listed for each parameter used as ±1 standard

**Table 5**
Stable isotope input data for components of the evaporation model.

| Lake | $\delta_{U\ (connecting\ channel\ inflow)}$ | | $\delta_{P\ (precipitation)}$ | | $\delta_{R\ (runoff)}$ | | $\delta_{A\ (atmospheric\ water)}$ | |
|---|---|---|---|---|---|---|---|---|
| | $\delta^{18}O$ | $\delta^2H$ | $\delta^{18}O$ | $\delta^2H$ | $\delta^{18}O$ | $\delta^2H$ | $\delta^{18}O$ | $\delta^2H$ |
| Superior | – | – | −11.74 ± 1 | −84.9 ± 9 | −12.50 ± 1 | −91.1 ± 9 | −24.3 ± 1 | −182 ± 9 |
| Huron | −7.09 ± 0.5 | −54.0 ± 4 | −10.33 ± 1 | −70.3 ± 9 | −10.80 ± 1 | −74.0 ± 9 | −22.1 ± 1 | −162 ± 9 |
| Michigan | −7.07 ± 0.7 | −53.9 ± 6 | −9.06 ± 1 | −62.1 ± 9 | −9.35 ± 1 | −64.3 ± 9 | −20.9 ± 1 | −155 ± 9 |
| Erie | −7.07 ± 0.3 | −53.9 ± 2 | −8.86 ± 1 | −57.4 ± 9 | −8.82 ± 1 | −57.4 ± 9 | −19.5 ± 1 | −127 ± 9 |
| Ontario | −6.52 ± 0.3 | −48.3 ± 2 | −10.15 ± 1 | −67.0 ± 9 | −10.53 ± 1 | −69.9 ± 9 | −21.1 ± 1 | −148 ± 9 |

**Table 6**
Evaporation model hydrologic inputs and hydroclimate data.

| Lake | $U$ (km³/year) | $P$ (km³/year) | $R$ (km³/year) | $O$ (km³/year) | $T_L$ (°C) | $T_A$ (°C) | $e$ (hPa) |
|---|---|---|---|---|---|---|---|
| Superior | – | 64 ± 19 | 50 ± 12 | 66 ± 7 | 4.9 ± 1 | 0.3 ± 1 | 4.7 ± 0.2 |
| Huron | 146 ± 33 | 52 ± 16 | 49 ± 12 | 208 ± 26 | 6.4 ± 1 | 6.5 ± 1 | 7.6 ± 0.3 |
| Michigan | 36 ± 12 | 55 ± 16 | 36 ± 9 | 88 ± 18 | 9.0 ± 1 | 5.8 ± 1 | 6.9 ± 0.3 |
| Erie | 172 ± 17 | 23 ± 7 | 19 ± 5 | 183 ± 13 | 15.0 ± 1 | 11.8 ± 1 | 10.3 ± 0.4 |
| Ontario | 183 ± 13 | 16 ± 5 | 34 ± 8 | 225 ± 4 | 9.4 ± 1 | 6.5 ± 1 | 7.4 ± 0.3 |

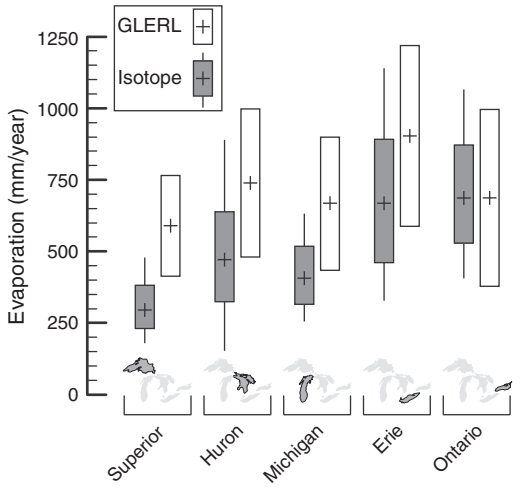


**Fig. 7.** Isotope mass balance (gray boxes) and evaporation estimates from the Great Lakes Environmental Research Laboratory (GLERL; white boxes; uncertainty from Neff and Nicholas, 2005) for the five North American Great Lakes. GLERL evaporation fluxes have been time-integrated (i.e., weighting of more recent years as more important) so that they may be compared with isotope-based evaporation estimates (except for Lake Superior where the 1948–2007 statistics were used). Isotope mass balance boxes represent 75th and 25th percentiles of Monte Carlo realizations (black lines extend to 10th and 90th percentiles) while crosses within boxes represent means.

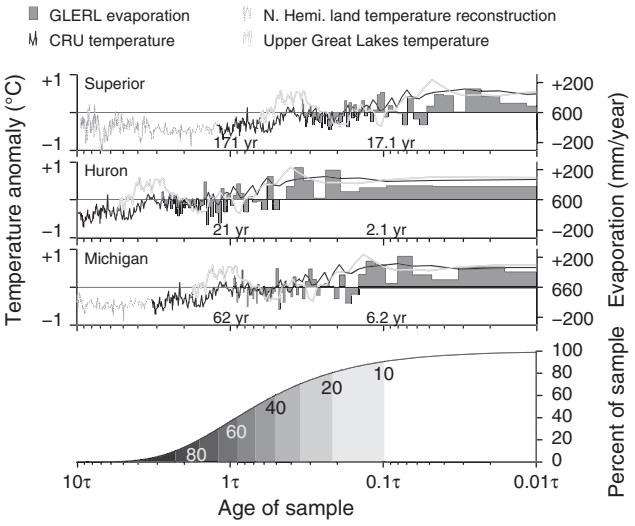


**Fig. 8.** Top panel: Great Lakes annual modeled evaporation rate from the Great Lakes Environmental Research Laboratory (gray bars) and atmospheric temperature anomaly (global temperature anomaly, black line: Climatic Research Unit: www.cru.uea.ac.uk; northern hemisphere proxy reconstruction of temperature anomaly, dark gray line: (Mann et al., 2008); average of long term measurements from 15 stations along the shores of Lakes Superior, Michigan and Huron, light gray line: data from National Climatic Data Center: www.ncdc.noaa.gov). Note that age scale (x axis) is logarithmic and scaled to each lake's residence time. Bottom panel: Water age distribution for a perfectly-mixed reservoir relative its residence time (τ). Grayscale bands mark 10% increments of reservoir water ages. The time-integration shown here highlights that a sample of water taken from a well-mixed reservoir contains water of different ages.

deviation. The evaporation calculation was then iterated many times to develop an uncertainty range for evaporation from each Great Lake.

## Results and discussion

Our stable-isotope-based evaporation results are shown in Fig. 7 along with long-term mean evaporation rates from the Great Lakes Environmental Research Laboratory (GLERL). Overall, evaporation uncertainties for our stable isotope approach are similar to GLERL model outputs (Neff and Nicholas, 2005) despite requiring only simple grab-sampling of lake water to assess evaporation fluxes over the lakes. Results for the five lakes range from 300 mm per year (Lake Superior) to ~450 mm per year (Michigan and Huron) to ~690 mm per year (Erie and Ontario). Downwind atmospheric moisture build-up over the Great Lakes is calculated by the values of $x$ required for model convergence (see Eq. (8)). Lakes Superior ($x = 40 \pm 8\%$) and Erie ($x = 40 \pm 7\%$) showed the highest amounts of downwind moisture build-up, followed by Lakes Michigan ($x = 33 \pm 8\%$), Ontario ($x = 27 \pm 10\%$) and Huron ($x = 15 \pm 9\%$). Stable-isotope-based evaporation rates overlap with modeled evaporation rates (GLERL) for all of the Great Lakes, except for Lake Superior where our calculated evaporation flux is about two-thirds of evaporation fluxes calculated in previous investigations (Table 7).

High moisture build-up over Lake Superior ($x = 40\%$) is explained by its large fetch of ~300 km and its headwater location where it receives air masses that have yet to travel over another large area of open water. The degree of atmospheric moisture build-up for each Great Lake shown here are in line with previous studies (Gat et al., 1994; Machavaram and Krishnamurthy, 1995), suggesting that Great Lakes evaporate accounts for between 10 and 40% of downwind atmospheric moisture, comparable to atmospheric moisture build-up over the western portion of the Mediterranean Sea of ~30% (Gat et al., 1996).

We reconcile Lake Superior's lower isotope-based evaporation flux relative to modern measurements (Spence et al., 2011) and modeling approaches (Croley, 1989: GLERL) by examining the age distribution of waters in Lake Superior. Atmospheric temperature anomaly data are presented in Fig. 8 (shown as relative to 1961–1990 mean, temperature data from Mann et al., 2008). The age distribution of a perfectly mixed reservoir relative to its residence time is shown in Fig. 8 (bottom graph). Lake Superior's residence time is 173 years (Quinn, 1992); therefore, about one third of the water within Lake Superior entered the lake under an older and different climate than that of the modern. To a lesser extent, this can also be seen in Lake Michigan, which has the second longest residence time of 62 years.

By integrating Northern Hemisphere temperature anomaly (Mann et al., 2008) over Superior's water age distribution (i.e., time elapsed since water entered the lake) we show that the lake water samples capture a −0.3 °C temperature anomaly compared to the 1948–2007 mean temperature (since the initiation of GLERL evaporation estimates; Fig. 8). Extrapolating a linear regression of average annual ice cover (Wang et al., 2012) and observed temperature anomaly for 16 stations in the upper Great Lakes region (Table 8) to a −0.3 °C temperature

**Table 7**
Comparison of various estimates of Great Lake annual evaporation rates in millimeters per year.

| | Isotope[a] | GLERL[b] | Morton (1967) | Schertzer (1978) | Derecki (1981) | Lofgren and Zhu (2000) | Blanken et al. (2011)[c] |
|---|---|---|---|---|---|---|---|
| Superior | 306 ± 76 | 590 ± 177 | 541 | 516 | 483 | 423 | 464, 645 |
| Huron | 483 ± 157 | 609 ± 213 | | | | 521 | |
| Michigan | 418 ± 101 | 646 ± 226 | | | | 445 | |
| Erie | 678 ± 215 | 903 ± 316 | | | 676 | 633 | |
| Ontario | 701 ± 171 | 663 ± 298 | 813 | | | 482 | |

[a] 75th and 25th percentiles of Monte Carlo analysis shown for isotope-based uncertainties.
[b] Uncertainty from Neff and Nicholas (2005).
[c] Values for 2008–2009 and 2009–2010 are shown.

**Table 8**
Temperature anomaly relative to 1961–1990 mean temperature for different time periods at monitored sites surrounding Lakes Superior, Huron and Michigan.

| Station | Lat. (°) | Lon. (°) | Alt (m.a.s.l.) | Mean temperature 1961–1990 | Temperature anomaly (relative to 1961–90 mean) | | |
|---|---|---|---|---|---|---|---|
| | | | | | 1901–1930 | 1931–1960 | 2000–2011 |
| Appleton | 44.25 | −88.36 | 229 | 7.37 °C | −0.34 | +0.16 | +0.38 |
| Cheboygan | 45.65 | −84.47 | 180 | 6.36 °C | −0.18 | +0.42 | +0.43 |
| East Tawas | 44.28 | −83.50 | 179 | 7.04 °C | −0.49 | +0.17 | +0.72 |
| Harbor Beach | 43.83 | −82.65 | 183 | 7.46 °C | +0.02 | +0.25 | −0.14 |
| Hart | 43.69 | −86.37 | 213 | 8.19 °C | −0.31 | +0.18 | +0.04 |
| Ironwood | 46.47 | −90.18 | 436 | 4.44 °C | +0.22 | +0.86 | +0.38 |
| Manistique | 45.95 | −86.25 | 189 | 5.09 °C | −0.10 | +0.68 | +0.76 |
| Manitowoc | 44.08 | −87.68 | 201 | 7.16 °C | −0.41 | +0.74 | +0.78 |
| Muskegon | 43.17 | −86.24 | 191 | 8.42 °C | −0.37 | +0.15 | +0.84 |
| Oconto | 44.88 | −87.95 | 201 | 6.25 °C | +0.26 | +0.91 | +0.66 |
| Oshkosh | 44.01 | −88.56 | 229 | 7.38 °C | −0.04 | +0.33 | +0.99 |
| Petoskey | 45.37 | −84.98 | 186 | 6.92 °C | −0.72 | +0.30 | +0.34 |
| Racine | 42.70 | −87.79 | 181 | 8.29 °C | +0.49 | +0.90 | +0.59 |
| Two Harbors | 47.03 | −91.67 | 191 | 4.56 °C | −0.33 | +0.27 | +0.82 |
| Waukesha | 43.01 | −88.23 | 253 | 8.20 °C | −0.40 | −0.06 | +0.05 |

anomaly, we find that Superior's isotopic signal integrates ~10% greater annual average ice cover than during the GLERL model time period, perhaps explaining a portion of the difference between the isotope-based and mass transfer (GLERL) evaporation rates. Projecting these findings into the future, there is a strong likelihood of similar increases in over-lake evaporation losses with warming over the coming decades.

## Concluding remarks

A new dataset of $\delta^{18}O$ and $\delta^{2}H$ for waters of the five North American Great Lakes is presented here. This dataset has been applied to a stable-isotope-based evaporation model that includes explicit consideration of lake effects on the atmosphere. Results show that uncertainties in the stable isotope approach are similar to those obtained from the mass transfer approach, and provide an evaporation estimate for the entire lake area rather than highly accurate, but site-specific fluxes, calculated using eddy covariance approach. A key feature of this analysis is that the isotope mass balance of Lake Superior (and perhaps Michigan) does not reflect present hydroclimatological conditions because long water residence time preserves the "memory" of a cooler past climate.

Supplementary data to this article can be found online at http://dx.doi.org/10.1016/j.jglr.2014.02.020.

## Acknowledgments

The authors express their gratitude to T. Johengen (University of Michigan), J. Adams and E. Osantowski (Environmental Protection Agency) for collecting water samples, to Tim Hunter for providing Great Lakes Environmental Research Laboratory data, to J. Welker for providing data from the U.S. Network for Isotopes in Precipitation, and to Paul Eby for analytical support. Support for this research was provided by Environment Canada and by an Industrial Postgraduate Scholarship awarded by the Natural Sciences and Engineering Research Council of Canada through the University of Waterloo and Alberta Innovates - Technology Futures to S. Jasechko.

## References

Aly, A.I.M., Froehlich, K., Nada, A., Awad, M., Hamza, M., Salom, W.M., 1993. Study of environmental isotope distribution in the Aswan High Dam Lake (Egypt) for estimation of evaporation of lake water and its recharge to adjacent groundwater. Environ. Geochem. Health 15, 37–49.
Angel, J.R., Kunkel, K.E., 2010. The response of Great Lakes water levels to future climate scenarios with an emphasis on Lake Michigan–Huron. J. Great Lakes Res. 36, 51–58.
Araguás-Araguás, L., Froehlich, K., Rozanski, K., 2000. Deuterium and oxygen-18 isotope composition of precipitation and atmospheric moisture. Hydrol. Process. 14, 1341–1355.
Assel, R., Cronk, K., Norton, D., 2003. Recent trends in Laurentian Great Lakes ice cover. Clim. Change 57, 185–204.
Bai, X., Wang, J., Sellinger, C., Clites, A., Assel, R.A., 2012. Interannual variability of Great Lakes ice cover and its relationship to NAO and ENSO. J. Geophys. Res. 117, C03002.
Barkan, E., Luz, B., 2007. Diffusivity fractionations of $H_2^{16}O/H_2^{17}O$ and $H_2^{16}O/H_2^{18}O$ in air and their implications for isotope hydrology. Rapid Commun. Mass Spectrom. 21, 2999–3005.
Benson, L.V., White, J.W.C., 1994. Stable isotopes of oxygen and hydrogen in the Truckee River–Pyramid Lake surface water system. 3. Source of water vapor overlying Pyramid Lake. Limnol. Oceanogr. 39, 1945–1958.
Birks, S.J., Edwards, T.W.D., 2009. Atmospheric circulation controls on precipitation isotope–climate relations in western Canada. Tellus 61, 566–576.
Birks, S.J., Gibson, J.J., 2009. Isotope hydrology research in Canada, 2003–2007. Can. Water. Resour. J. 34, 163–176.
Blanken, P.D., Spence, C., Hedstrorn, N., Lenters, J.D., 2011. Evaporation from Lake Superior: 1: Physical controls and processes. J. Great Lakes Res. 37, 707–716.
Bolsenga, S.J., Norton, D.C., 1993. Great Lakes air temperature trends for land stations, 1901–1987. J. Great Lakes Res. 19, 379–388.
Bowen, G.J., Revenaugh, J., 2003. Interpolating the isotopic composition of modern meteoric precipitation. Water Resour. Res. 39, 1299.
Bowen, G.J., Wilkinson, B., 2002. Spatial distribution of $\delta^{18}O$ in meteoric precipitation. Geology 30, 315–318.
Bowen, G.J., Kennedy, C.D., Henne, P.D., Zhang, T., 2012. Footprint of recycled water subsidies downwind of Lake Michigan. Ecosphere 3, 1–16.
Brock, B.E., Yi, Y., Clogg-Wright, K.P., Edwards, T.W.D., Wolfe, B.B., 2009. Multi-year landscape-scale assessment of lakewater balances in the Slave River Delta, NWT, using water isotope tracers. J. Hydrol. 379, 81–91.
Brown, R.M., 1970. Environmental isotope variations in the precipitation, surface waters and in tree rings in Canada. Interpretation of Environmental Isotope Data in Hydrology. Int. Atomic Energy Agency, Vienna, pp. 4–6.
Buck, A.L., 1981. New equations for computing vapor pressure and enhancement factor. J. Appl. Meteorol. 20, 1527–1532.
Cappa, C.D., Hendricks, M.B., DePaolo, D.J., Cohen, R.C., 2003. Isotopic fractionation of water during evaporation. J. Geophys. Res. Atmos. 108, 4525–4535.
Chapra, S.C., Dove, A., Rockwell, D.C., 2009. Great Lakes chloride trends: long-term mass balance and loading analysis. J. Great Lakes Res. 35, 273–284.
Coplen, T.B., 1996. New guidelines for reporting stable hydrogen, carbon, and oxygen isotope-ratio data. Geochim. Cosmochim. Acta 60, 3359–3360.
Craig, H., 1961. Isotopic variations in meteoric waters. Science 133, 1702–1703.
Craig, H., 1975. Lake Tanganyika Geochemical and Hydrographic Study: 1973 Expedition. Scripps Institute of Oceanography (Reference 75–5, La Jolla, California, 83 pp.).
Craig, H., Gordon, L.I., 1965. Deuterium and oxygen-18 variations in the ocean and the marine atmosphere. In: Tongiorgi, E. (Ed.), Proceedings of a Conference on Stable Isotopes in Oceanographic Studies and Paleotemperatures. Spoleto, Italy, pp. 9–130.
Croley, T.E., 1989. Verifiable evaporation modeling on the Laurentian Great Lakes. Water Resour. Res. 25, 781–792.
Croley, T.E., Assel, R.A., 1994. A one-dimensional ice thermodynamics model for the Laurentian Great Lakes. Water Resour. Res. 30, 625–639.
Dansgaard, W., 1964. Stable isotopes in precipitation. Tellus 16, 436–468.
Derecki, J.A., 1981. Stability effects on Great Lakes evaporation. J. Great Lakes Res. 7, 357–362.
Dinçer, T., Hutton, L.G., Khupe, B.B.J., 1978. Study, using stable isotopes, of flow distribution, surface–groundwater relations and evapotranspiration in the Okavango Swamp, Botswana. Isotope Hydrology 1978. Int. Atomic Energy Agency, Vienna, pp. 3–26.
Ehhalt, D., Knott, K., 1965. Kinetische Isotopentrennung bei der Verdampfung von Wasser. Tellus 17, 389–397.
Eichenlaub, V.L., 1970. Lake effect snowfall to the lee of the Great Lakes: its role in Michigan. Bull. Am. Meteorol. Soc. 51, 403–473.
Epstein, S., Mayeda, T., 1953. Variation of $O^{18}$ content of waters from natural sources. Geochim. Cosmochim. Acta 4, 213–224.
Fontes, J.-C.h., Gonfiantini, R., 1970. Composition isotopique et origine de la vapeur d'eau atmospherique dans la region du lac Leman. Earth Planet. Sci. Lett. 7, 325–329.

Fontes, J.-C.h., Gonfiantini, R., Roche, M.A., 1970. Deutérium et oxygène-18 dans les eaux du lac Tchad, *in* Isotope Hydrology 1970. Int. Atomic Energy Agency, Vienna 387–404.
Gat, J.R., 1996. Oxygen and hydrogen isotopes in the hydrologic cycle. Annu. Rev. Earth Planet. Sci. 24, 225–262.
Gat, J.R., Bowser, C.J., Kendall, C., 1994. The contribution of evaporation from the Great Lakes to the continental atmosphere: estimate based on stable isotope data. Geophys. Res. Lett. 21, 557–560.
Gat, J.R., Shemesh, A., Tziperman, E., Hecht, A., Georgopoulos, D., Basturk, O., 1996. The stable isotope composition of waters of the eastern Mediterranean Sea. J. Geophys. Res. 101, 6441–6451.
Gibson, J.J., Edwards, T.W.D., 2002. Regional water balance trends and evaporation–transpiration partitioning from a stable isotope survey of lakes in northern Canada. Global Biogeochem. Cycles 16, 1026.
Gibson, J.J., Birks, S.J., Edwards, T.W.D., 2008. Global prediction of $\delta_A$ and $\delta^2H$-$\delta^{18}O$ evaporation slopes for lakes and soil water accounting for seasonality. Global Biogeochem. Cycles 22, GB2031.
Gilath, C., Gonfiantini, R., 1983. Lake dynamics. In: Mortimer, C.H. (Ed.), Guidebook on Nuclear Techniques in Hydrology. Tech. Rep. Ser., 91. Int. At. Energy Agency, Vienna, pp. 129–161.
Gonfiantini, R., Zuppi, G.M., Eccles, D.H., Ferro, W., 1979. Isotope investigation of Lake Malawi. In: Mortimer, C.H. (Ed.), Isotopes in Lake Studies. International Atomic Energy Agency, Vienna, pp. 195–207.
Hanrahan, J.L., Kravtsov, S.V., Roebber, P.J., 2010. Connecting past and present climate variability to the water levels of Lakes Michigan and Huron. Geophys. Res. Lett. 37, L01701.
Hayhoe, K., VanDorn, J., Croley, T., Schlegal, N., Wuebbles, D., 2010. Regional climate change projections for Chicago and the US Great Lakes. J. Great Lakes Res. 36, 7–21.
Horita, J., Wesolowski, D.J., 1994. Liquid–vapor fractionation of oxygen and hydrogen isotopes of water from the freezing to the critical temperature. Geochim. Cosmochim. Acta 58, 3425–3437.
Horita, J., Rozanski, K., Cohen, S., 2008. Isotope effects in the evaporation of water: a status report of the Craig–Gordon model. Isot. Environ. Health Stud. 44, 23–49.
Jasechko, S., Sharp, Z.D., Gibson, J.J., Birks, S.J., Yi, Y., Fawcett, P.J., 2013. Terrestrial water fluxes dominated by transpiration. Nature 496, 347–350.
Kabeya, N., Kubota, T., Shimizu, A., Nobuhiro, T., Tsuboyama, Y., Chann, S., Tith, N., 2008. Isotopic investigation of river water mixing around the confluence of the Tonle Sap and Mekong rivers. Hydrol. Process. 22, 1351–1358.
Karim, A., Veizer, J., Barth, J., 2008. Net ecosystem production in the great lakes basin and its implications for the North American missing carbon sink: a hydrologic and stable isotope approach. Global Planet. Change 61, 15–27.
Kendall, C., Coplen, T.B., 2001. Distribution of oxygen-18 and deuterium in river waters across the United States. Hydrol. Process. 15, 1363–1393.
Kutzbach, J.E., Williams, J.W., Vavrus, S.J., 2005. Simulated 21st century changes in regional water balance of the Great Lakes region and links to changes in global temperature and poleward moisture transport. Geophys. Res. Lett. 32, L17707.
Lofgren, B.M., Zhu, Y.C., 2000. Surface energy fluxes on the Great Lakes based on satellite-observed surface temperatures 1992 to 1995. J. Great Lakes Res. 26, 305–314.
Longinelli, A., Stenni, B., Genoni, L., Flora, O., Defrancesco, C., Pellegrini, G., 2008. A stable isotope study of the Garda lake, Northern Italy: its hydrological balance. J. Hydrol. 360, 103–116.
Machavaram, M.V., Krishnamurthy, R.V., 1995. Earth surface evaporative process: a case study from the Great Lakes region of the United States based on deuterium excess in precipitation. Geochim. Cosmochim. Acta 59, 4279–4283.
Magnuson, J.J., Webster, K.E., Assel, R.A., Bowser, C.J., Dillin, P.J., Eaton, J.G., Evans, H.E., Fee, E.J., Hall, R.I., Mortsch, L.R., Schindler, D.W., Quinn, F.H., 1997. Potential effects of climate changes on aquatic systems: Laurentian Great Lakes and Precambrian Shield region. Hydrol. Process. 11, 825–871.
Mann, M.E., Zhang, Z., Hughes, M.K., Bradley, R.S., Miller, S.K., Rutherford, S., Ni, F., 2008. Proxy-based reconstructions of hemispheric and global surface temperature variations over the past two millennia. Proc. Natl. Acad. Sci. U. S. A. 105, 13252–13257.
McKenna, S.A., Ingraham, N.L., Jacobson, R.L., Cochran, G.F., 1992. A stable isotope study of bank storage mechanisms in the Truckee river basin. J. Hydrol. 134, 203–219.
Mesinger, F., DiMego, G., Kalnay, E., Shafran, P., Ebisuzaki, W., Jovic, D., Woollen, J., Mitchell, K., Rogers, E., Ek, M., Fan, Y., Grumbine, R., Higgins, W., Li, H., Lin, Y., Manikin, G., Parrish, D., Shi, W., 2005. North American Regional Reanalysis. Bull. Am. Meteorol. Soc. 87, 343–360.
Morrison, J., Brockwell, T., Merren, T., Fourel, F., Phillips, A.M., 2001. A new on-line method for high precision stable hydrogen isotopic analyses on nanolitre water samples. Anal. Chem. 73, 3570–3575.
Morton, F.I., 1967. Evaporation from large deep lakes. Water Resour. Res. 3, 181–200.
Neff, B.P., Nicholas, J.R., 2005. Uncertainty in Great Lakes water balance. U. S. Geological Survey Scientific Investigations Report 2004–5100 (42 pp.).
New, M., Lister, D., Hulme, M., Makin, I., 2002. A high-resolution data set of surface climate over global land areas. Clim. Res. 21, 1–25.
Oberhänsli, H., Weise, S.M., Stanichny, S., 2009. Oxygen and hydrogen isotopic water characteristics of the Aral Sea, Central Asia. J. Mar. Syst. 76, 310–321.
Quinn, F.H., 1992. Hydraulic residence times for the Laurentian Great Lakes. J. Great Lakes Res. 18, 22–28.
Rasmusen, E.M., 1968. Atmospheric water vapour transport and the water balance of North America. Part II large-scale water balance investigations. Mon. Weather Rev. 96, 720–734.
Ricketts, R.D., Johnson, T.C., 1996. Climate change in the Turkana basin as deduced from a 4000 year long $\delta^{18}O$ record. Earth Planet. Sci. Lett. 142, 7–17.
Rozanski, K., Araguás-Araguás, L., Gonfiantini, R., 1993. Isotopic patterns in modern global precipitation. In: Swart, P.K., McKenzie, J., Lohmann, K.C., Savin, S. (Eds.), Climate Change in Continental Isotopic Records, Geophysical Monograph Series 78. American Geophysical Union, Washington DC, pp. 1–36.
Russell, J.M., Johnson, T.C., 2006. The water balance and stable isotope hydrology of Lake Edward, Uganda–Congo. J. Great Lakes Res. 32, 77–90.
Schertzer, W.M., 1978. Energy budget and monthly evaporation estimates for Lake Superior, 1973. J. Great Lakes Res. 4, 320–330.
Seal, R.R., Shanks, W.C., 1998. Oxygen and hydrogen isotope systematics of Lake Baikal, Siberia: implications for paleoclimate studies. Limnol. Oceanogr. 43, 1251–1261.
Spence, C., Blanken, P.D., Hedstrom, N., Fortin, V., Wilson, H., 2011. Evaporation from Lake Superior: 2: spatial distribution and variability. J. Great Lakes Res. 37, 717–724.
Stewart, M.K., 1975. Stable isotope fractionation due to evaporation and isotopic-exchange of falling water drops: applications to atmospheric processes and evaporation of lakes. J. Geophys. Res. 80, 1133–1146.
Taniguchi, M., Nakayama, T., Tase, N., Shimada, J., 2000. Stable isotope studies of precipitation and river water in the Lake Biwa basin, Japan. Hydrol. Process. 14, 539–556.
Vogt, H.J., 1976. Isotopentrennung bei der Verdampfung von Wasser. Universität Heidelberg, Staatsexamensarbeit (78 pp.).
Wang, J., Bai, X., Hu, H., Clites, A., Colton, M., Lofgren, B., 2012. Temporal and spatial variability of Great Lakes ice cover, 1973–2010. J. Clim. 25, 1318–1329.
Wassenaar, L.I., Athanasopoulos, P., Hendry, M.J., 2011. Isotope hydrology of precipitation, surface and ground waters in the Okanagan Valley, British Columbia, Canada. J. Hydrol. 411, 37–48.
Welker, J.M., 2000. Isotopic ($\delta^{18}O$) characteristics of weekly precipitation collected across the USA: an initial analysis with application to water source studies. Hydrol. Process. 14, 1449–1464.
Yi, Y., Brock, B.E., Falcone, M.D., Wolfe, B.B., Edwards, T.W.D., 2008. A coupled isotope tracer method to characterize input water to lakes. J. Hydrol. 350, 1–13.
Zuber, A., 1983. On the environmental isotope method for determining the water balance of some lakes. J. Hydrol. 61, 409–427.